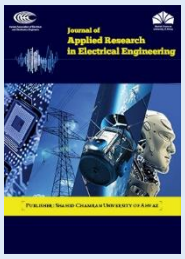
Shahid Chamran University of Ahvaz

Iranian Association of Electrical and Electronics Engineers

Journal of Applied Research in Electrical Engineering

E-ISSN: 2783-2864
P-ISSN: 2717-414X
Homepage: https://jaree.scu.ac.ir/



Research Article

Pitch Blade Regulation of Wind Turbines Using Dynamic Sliding Mode Control and Nonlinear Sliding Observer

Ali Karami-Mollaee*

Faculty of Electrical and Computer Engineering, Hakim Sabzevari University, Sabzevar, Iran

** Corresponding Author: karami@hsu.ac.ir*

Abstract: Wind turbines (WTs), particularly those with two-shaft drivetrain and variable speed, present a complex model. This study initially shifts all WT variables to the low-speed shaft. Subsequently, the Taylor series for the torque is generated by the wind, or rotor torque, is computed near the optimal blades pitch angle and the optimal blades tip speed ratio (TSR). At these optimal points, wind power extraction is maximized, i.e. maximum power point tracking (MPPT) is achieved. The paper introduces two novel state feedbacks and derives a linear model with uncertainty, represented by a new input variable. This uncertainty can lead to mechanical stress, particularly if the new input variable lacks smoothness. To address these issues, a robust sliding mode controller using a dynamic approach (D-SMC) is employed, which eliminates chattering through a low-pass integrator. The sliding surface dimension in D-SMC exceeds with respect of the original system, necessitating the estimation of this newly introduced state. Therefore, the paper proposes a new sliding observer with a nonlinear approach (NSO). The stability of the both D-SMC and NSO is verified using Lyapunov theory. The superiority of D-SMC is demonstrated by comparing to the conventional sliding mode controller (C-SMC) under identical NSO and simulation conditions.

Keywords: Nonlinear sliding observer, pitch angle control, sliding mode control, wind turbine.

Article history
Received 08 April 2025; Revised 20 January 2026; Accepted 27 January 2026; Published online 29 July 2026.
© 2026 Published by Shahid Chamran University of Ahvaz & Iranian Association of Electrical and Electronics Engineers (IAEEE)
How to cite this article
A. Karami-Mollaee, " Pitch Blade Regulation of Wind Turbines Using Dynamic Sliding Mode Control and Nonlinear Sliding Observer," *J. Appl. Res. Electr. Eng.*, vol. 4, no. 2, pp. 205-215, 2025. DOI: https://doi.org/10.22055/jaree.2026.49363.1191

Check for updates

1. INTRODUCTION

The escalating global warming from fossil fuel, significant effort strides in harnessing sustainable renewable energy sources like solar [1] and wind [2,3]. These energy forms not only are environmentally but also are globally available in all of the countries [4]. Energy of wind, in particular, has very interested due to the cost-effective operation of WTs [5,6]. The wind power is converted to the rotational torque for generators, using WT. Consequently, two main types of WTs have emerged: fixed-speed (FS) [7,8] and variable-speed (VS) [9]. FS kinds fail to capture the maximum of wind power across varying wind speeds (WSs) [10], leading to the development of VS kinds [11]. VS kinds optimize power capture by dividing operational performance into two regions based on WS, known as rated [11]. Below this rated WS, generator torque is used to maximize power extraction, while above it, turbine blade pitch angle sets as the control input [12,13]. Moreover, there exist two others critical WSs, cut-in and cut-out, which are important in turbine operation modes. Outside this range, turbines cease operation to avoid economic loss and structural fatigue [14].

Numerous control strategies have been proposed for the region between rated and cut-out speeds, focusing on pitch angle regulation [12-22]. However, mechanical stress remains a significant challenge for WTs due to the uncertainty [23]. To mitigate these stresses, a robust controller is essential to handle drivetrain uncertainties [23]. Despite various available approaches, many controllers cannot exhibit robustness; for instance, classical controllers like proportional-integral-derivative (PID) [13,17,19], PID with adaptive self-tuning regulator (STR) [15], a gain scheduled PID [16] or a PI scheme of controller [21]. Adaptive and PI combination is in [20], or some feedback controller are proposed in [18,22].

Among these, sliding mode control (SMC) stands for its ability to counteract mechanical stresses due to its invariance

property [23], a feature even more stronger than robustness [24-26]. Hence, many researches have concentrated on sliding mode pitch control [27-33].

But, SMC is suffered by chattering, a detrimental phenomenon due to the Sign function using [24-26]. To address chattering suppression, some approaches have been introduced [34]: methodologies like boundary layer [35,36], adaptive boundary layer [37,38], higher order [39,40], and dynamic based approach (D-SMC) [25,41-43]. Boundary layer and adaptive boundary layer, however, cannot reserve the most characteristic of SMC, i.e. invariance [24-26]. Higher order uses more derivatives of system function, needs observers for their estimation [44-48].

D-SMC, on the other hand, employs a low-pass-integrator filter to mitigate the Sign function discontinuity, leading to an increase in system states [42]. Controlling this expanded system (system plus integrator) demands a capable observer to estimate the system model [25]. Then in higher order, system function differentiations are used but in dynamic approach just an added state is needed and this is its preference.

The primary goal of an observer is to use known system outputs and inputs to estimate unmeasurable system components. Usually the observer output, alongside the main system, is utilized for feedback to correct the observer parameters [49-55]. Identification concept spans of a vast structure in literature such as state observer [49,50], disturbance observer [51] and model identification [25,52,53]. Sliding observers are particularly valued for their straightforward implementation and robustness against uncertainties [54,55].

Motivated by the persistent issue of chattering and based on the disadvantages of boundary and adaptive boundary layer and higher order, a new D-SMC approach is proposed for pitch angle regulation in WTs. D-SMC reliably eliminate chattering, while maintain the invariance property, causes alleviation of mechanical stresses. Additionally, a novel NSO is developed for controller implementation and plant model identification. The D-SMC and the NSO stability are substantiated through Lyapunov stability theory.

Therefore, the overall contribution of this paper can be summarized as follow:

1. A new MPPT approach is implemented to VS wind turbine.
2. A new structure of robust D-SMC is proposed.
3. The chattering is removed using D-SMC.
4. A smooth input control is obtained for pitch angle of WT.
5. A new scheme of NSO is proposed to estimate the unknown uncertain.

The methodology is demonstrated in seven categories. Initially, the WT model and problem formulation are outlined in sections 2 and 3. Subsequently, section 4 introduces the novel NSO and its stability. Section 5 is dedicated to comparative analysis and control design. Section 6 shows simulations to validate the proposed method superiority. The paper conclusion is provided in section 7.

2. Complete Model of Wind Turbine

A WT has three series subsystems, aerodynamic, mechanical drivetrain and generator [23,29] as in Fig. 1.

2.1. Aerodynamic Structure

The formula of captured power by WT, is a function of the surface coverage by blades i.e. $r^2\pi$ (r is the blade length), WS i.e $v(t)$, air density i.e. ρ, and C_p as the power coefficient [43].

$$P_a = \frac{\rho\pi r^2 v^2}{2} C_p(\beta,\lambda) \tag{1}$$

In which, λ is (TSR), ω_r and β are angular velocity of rotor side and pitch blade respectively.

$$\lambda = \frac{r\omega_r}{v} \tag{2}$$

Note that C_p commonly written as the following equation [23].

$$\begin{aligned} C_p(\beta,\lambda) &= \left(\frac{\rho_1\rho_2}{\rho_i} - \rho_1\rho_3\beta - \rho_1\rho_4\right) e^{-\frac{\rho_5}{\rho_i}} + \rho_6\lambda \\ \frac{1}{\rho_i} &= -\frac{0.035}{\beta^3+1} + \frac{1}{\lambda+0.08\beta} \end{aligned} \tag{3}$$

such that:

$$\begin{aligned} &\rho_1 = 0.5176, \rho_2 = 116, \rho_3 = 0.4 \\ &\rho_4 = 5, \rho_5 = 21, \rho_6 = 0.0067 \end{aligned} \tag{4}$$

The rotor torque produced by the wind is also satisfied $P_a = T_a\omega_r$, therefore:

$$T_a = \frac{C_p}{2\lambda}\rho\pi r^3 v^2 \tag{5}$$

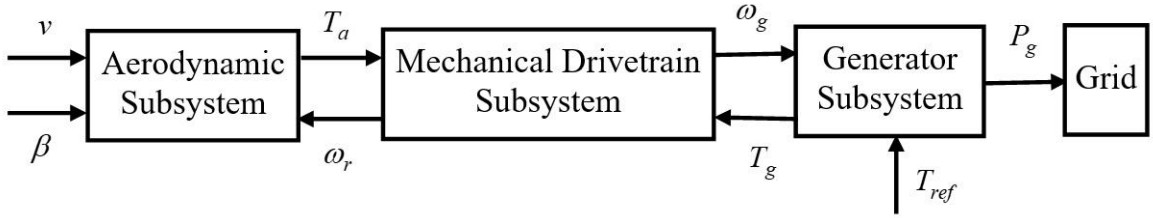


Fig. 1: The complete model of a wind turbine

2.2. Mechanical Structure

By definition of J_r and J_g as the rotor and generator inertia respectively, the two-shaft drivetrain is formulated as the following equations [56], which is shown in Fig. 2.

$$\begin{aligned} J_r\dot{\omega}_r &= -K_r\omega_r + T_a - T_{ls} \\ J_g\dot{\omega}_g &= -K_g\omega_g - T_g + T_{hs} \end{aligned} \tag{6}$$

Moreover, T_a and T_g are the outputs of the rotor torque and the generator torque respectively, imposed to the drivetrain. Constants K_r and K_g are the external dapping of rotor and generator side. In the low-speed shaft, braking torque is a function of ω_r and ω_g i.e. angular velocity of rotor and generator.

$$T_{ls} = K_{ls}(\omega_r - \omega_{ls}) + B_{ls}(\theta_r - \theta_{ls}) \tag{7}$$

The low-speed shaft parameters θ_{ls}, θ_r, K_{ls}, B_{ls}, and ω_{ls} are deviation of angular speed of, deviation of rotor side speed, low-speed of shaft damping, shaft stiffness, and angular velocity of deviation respectively, and the gearbox ratio is as:

$$n_g = \frac{\omega_g}{\omega_r} = \frac{T_{ls}}{T_{hs}} \tag{8}$$

Now using (6) and (8) results:

$$J_g\left(n_g\dot{\omega}_r\right) = -K_g\left(n_g\omega_r\right) - T_g + \left(\frac{T_{ls}}{n_g}\right) \tag{9}$$

or:

$$n_g{}^2 J_g\dot{\omega}_r = -n_g{}^2 K_g\omega_r - n_g T_g + T_{ls} \tag{10}$$

By definition of $J_t = J_r + n_g{}^2 J_g$ and $K_t = K_r + n_g{}^2 K_g$ and using (10) and the first part of (6), one can conclude the low-speed shaft formula as:

$$J_t\dot{\omega}_r = -K_t\omega_r + T_a - n_g T_g \tag{11}$$

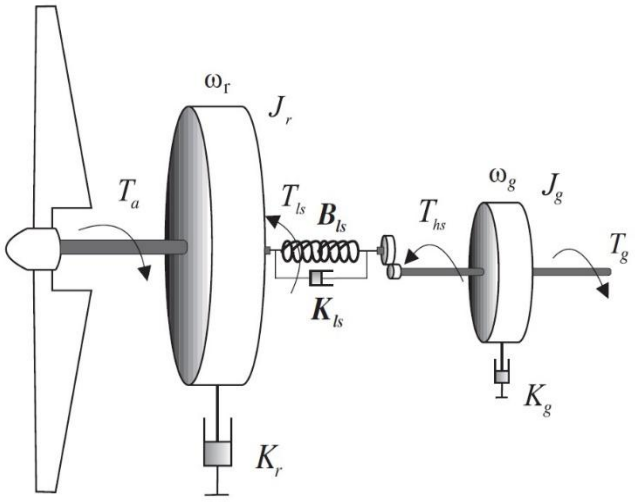


Fig. 2: The two-shaft drivetrain structure

2.3. Generator Dynamic Structure

Suppose T_g be the output torque of generator with the time constant $\tau_g = 15s$ and reference torque of T_{ref}, then one have:

$$\dot{T}_g = \frac{T_{ref} - T_g}{\tau_g} \tag{12}$$

The power that is injected into the grid is as:

$$P_g = \eta_g\omega_g T_g \tag{13}$$

In which η_g is the generator efficiency.

3. Problem Formulation

Consider the derivative of $C_p(\beta,\lambda)$ with respect to β.

$$\begin{aligned} \frac{dC_p}{d\beta} &= \frac{\partial C_p}{\partial\rho_i}\frac{\partial\rho_i}{\partial\beta} + \frac{\partial C_p}{\partial\beta} \\ &= \left(-\frac{\rho_1\rho_2}{\rho_i^2} + \frac{\rho_1\rho_2\rho_5}{\rho_i^3} - \frac{\rho_1\rho_3\rho_5\beta}{\rho_i^2} - \frac{\rho_1\rho_4\rho_5}{\rho_i^2}\right) \\ &\times\left(\frac{-0.08}{(\lambda+0.08\beta)^2} + \frac{0.035}{(\beta^3+1)^2}\right)e^{-\frac{\rho_5}{\rho_i}} - \rho_1\rho_3 e^{-\frac{\rho_5}{\rho_i}} \end{aligned} \tag{14}$$

Then the Taylor series of rotor torque (5) results:

$$T_a = \frac{\rho\pi r^3 v^2}{2\lambda_{opt}}\left.\frac{dC_p}{d\beta}\right|_{\substack{\beta=\beta_{opt}\\ \lambda=\lambda_{opt}}}(\beta-\beta_{opt}) + HOT \tag{15}$$

where $(\beta_{opt},\lambda_{opt})$ is optimal operation point and HOT is the higher order terms in Taylor series.

Therefore, the linearized model of (11) will be as follows:

$$\begin{aligned} \dot{\omega}_r &= -\frac{K_t}{J_t}\omega_r - \frac{n_g}{J_t}T_g + \frac{T_a}{J_t} \\ &= -\frac{K_t}{J_t}\omega_r - \frac{n_g}{J_t}T_g \\ &+ \frac{\rho\pi r^3 v^2}{2J_t\lambda_{opt}}\left.\frac{dC_p}{d\beta}\right|_{\substack{\beta=\beta_{opt}\\ \lambda=\lambda_{opt}}}(\beta-\beta_{opt}) + \Delta \end{aligned} \tag{16}$$

and Δ is the unknown uncertainty.

$$\Delta = \frac{HOT}{J_t} \tag{17}$$

The uncertainty Δ is bounded, because around the optimal operation points the Taylor series converge.

$$|\Delta| \le \eta \tag{18}$$

Using the new input signal $u \in R^{1\times1}$, the following state feedback is provided:

$$\beta = \frac{\left(\frac{K_t}{J_t}+a_2\right)\omega_r + \left(\frac{n_g}{J_t}+a_1\right)T_g + u}{\frac{\rho\pi r^3 v^2}{2J_t\lambda_{opt}}\frac{dC_p}{d\beta}\Big|_{\substack{\beta=\beta_{opt}\\ \lambda=\lambda_{opt}}}} + \beta_{opt} \tag{19}$$

and therefore:

$$\dot{\omega}_r = +a_1 T_g + a_2\omega_r + u + \Delta \tag{20}$$

Consider a reference feedback for the generator torque (13):

$$T_{ref} = \tau_g\omega_r + T_g \tag{21}$$

therefore:

$$\dot{T}_g = \omega_r \tag{22}$$

By definition of the state variables $x_1 = T_g$ and $x_2 = \omega_r$ with the state vector $x = [x_1, x_2]$ one can write:

$$\dot{x} = Ax + Bu + B\Delta \tag{23}$$

whereas:

$$A = \begin{bmatrix} 0 & 1 \\ a_1 & a_2 \end{bmatrix},\ B = \begin{bmatrix} 0 \\ 1 \end{bmatrix} \tag{24}$$

Suppose the numbers a_1 and a_2 are chosen such that matrix A be Hurwitz and satisfied the following Lyapunov equality equation [24]:

$$Q = -\left(PA + A^T P\right) \tag{25}$$

Such that the arbitrary matrixes $Q \in R^{n\times n}$ and $P \in R^{n\times n}$ are symmetric positive definite [24]. To design the chattering-free D-SMC with the desired signals $x_d = [x_{d1}, x_{d2}]$ and x_{d3}, the following sliding surface is defined.

$$\begin{aligned} s &= \lambda(x - x_d) + \lambda_3(x_3 - x_{d3}) \\ \lambda &= [\lambda_1, \lambda_2] \end{aligned} \tag{26}$$

where $x_3 = \dot{x}_2$, and coefficients $\lambda_i : i = 1,2,3$ are chosen such that the states variables $x_i : i = 1,2,3$ converge to zero when $s = 0$. Unfortunately the augmented state variable $x_3 = \dot{x}_2 = a_1x_1 + a_2x_2 + u + \Delta$ is not known due to uncertain parameter Δ. Hence, to the following new sliding observer structure is proposed for the system (23) in the next section.

Remark 1- if the system does not have the uncertainty, the need of observer is removed. Because in this case the variable $x_3 = \dot{x}_2$ are available and accessible.

4. Nonlinear Sliding Observer Structure

Consider the following NSO with inputs $\mu_i : i = 1,2$:

$$\begin{cases} \dot{\hat{x}}(t) = \mu_2(t) + z(t) + A\hat{x} + Bu + B\eta \\ \dot{z}(t) = \mu_1(t) - z(t) \end{cases} \tag{27}$$

where $\hat{x}(t) = [\hat{x}_1, \hat{x}_2]^T$ and $z(t) = [z_1, z_2]^T$ are state estimation vector of the system and the auxiliary vector signal.

Theorem 1- With the following NSO inputs, error estimation $e = x - \hat{x}$ converges to zero.

$$\begin{aligned} \mu_1 &= e \in R^{2\times 1} \\ \mu_2 &= P^{-1}sign(e) \in R^{2\times 1} \end{aligned} \tag{28}$$

Proof. The dynamic of the error can be written as:

$$\dot{e}(t) = -\mu_2(t) - z(t) + Ae - B\eta + B\Delta \tag{29}$$

Consider a Lyapunov function as:

$$V(t) = \frac{1}{2}z(t)^T Pz(t) + \frac{1}{2}e(t)^T Pe(t) \tag{30}$$

then:

$$\dot{V} = \frac{1}{2}\dot{z}^T Pz + \frac{1}{2}z^T P\dot{z} + \frac{1}{2}\dot{e}^T Pe + \frac{1}{2}e^T P\dot{e} \tag{31}$$

The first part of the observer (27) Results that:

$$\begin{aligned} \dot{V} &= \frac{1}{2}(\mu_1 - z)^T Pz + \frac{1}{2}z^T P(\mu_1 - z) \\ &\quad + \frac{1}{2}\dot{e}^T Pe + \frac{1}{2}e^T P\dot{e} \end{aligned} \tag{32}$$

or:

$$\begin{aligned} \dot{V} &= \frac{1}{2}(-z + \mu_1)^T Pz + \frac{1}{2}z^T P(-z + \mu_1) \\ &\quad + \frac{1}{2}\dot{e}^T Pe + \frac{1}{2}e^T P\dot{e} \\ &= -z^T Pz + \frac{1}{2}\mu_1{}^T Pz + \frac{1}{2}z^T P\mu_1 + \frac{1}{2}\dot{e}^T Pe + \frac{1}{2}e^T P\dot{e} \\ &= -z^T Pz + \mu_1{}^T Pz + + \frac{1}{2}\dot{e}^T Pe + \frac{1}{2}e^T P\dot{e} \end{aligned} \tag{33}$$

Using (29) leads to:

$$\begin{aligned} \dot{V} &= -z^T Pz + \mu_1{}^T Pz \\ &\quad + \frac{1}{2}(-z + Ae + B\Delta - B\eta - \mu_2)^T Pe \\ &\quad + \frac{1}{2}e^T P(-z + Ae + B\Delta - B\eta - \mu_2) \end{aligned} \tag{34}$$

or:

$$\begin{aligned} \dot{V} &= -z^T Pz + \mu_1{}^T Pz - \frac{1}{2}z^T Pe + \frac{1}{2}e^T A^T Pe \\ &\quad + \frac{1}{2}(B\Delta - B\eta)^T Pe - \frac{1}{2}\mu_2{}^T Pe - \frac{1}{2}e^T Pz + \frac{1}{2}e^T PAe \\ &\quad + \frac{1}{2}e^T P(B\Delta - B\eta) - \frac{1}{2}e^T P\mu_2 \\ &= -z^T Pz + \mu_1{}^T Pz - e^T Pz + \frac{1}{2}e^T\left(PA + A^T P\right)e \\ &\quad + e^T P(B\Delta - B\eta) - e^T P\mu_2 \end{aligned} \tag{35}$$

Using (18) and (25) follows that:

$$\dot{V} \le -z^T Pz + \mu_1{}^T Pz - e^T Pz - \frac{1}{2} e^T Qe - e^T P\mu_2 \tag{36}$$

Now replace the observer inputs (28) into (36):

$$\begin{aligned}\dot{V} &\le -z^T Pz + e^T Pz - e^T Pz - \frac{1}{2} e^T Qe \\ &\quad - e^T PP^{-1} sign(e) \\ &= -z^T Pz - \frac{1}{2} e^T Qe - e^T sign(e) \\ &= -z^T Pz - \frac{1}{2} e^T Qe - \sum_{i=1}^{3} |e_i|\end{aligned} \tag{37}$$

or:

$$V \le -z^T Pz - \frac{1}{2} e^T Qe \tag{38}$$

Consequently, the observer error vector and auxiliary vector converge to zero.

5. Dynamic Sliding Mode Control Structure

To overcome on the uncertain model and also suppress the chattering D-SMC is constructed. The effective performance is shown with comparison to C-SMC. Due to the using the same observer (27) in both approaches, comparison is comprehensive.

5.1. Proposed Dynamic Controller

According to the previous illustrations and formulas, the proposed D-SMC diagram is shown in Fig. 3.

Consider the estimation of sliding surface (26):

$$\begin{aligned}s &= \lambda(\hat{x} - x_d) + \lambda_3(\hat{x}_3 - x_{d3}) \\ &= \lambda\hat{x} + \lambda_3\hat{x}_3 - \lambda x_d - \lambda_3 x_{d3}\end{aligned} \tag{39}$$

By defining the vector of $F = [0,1] \in R^{1\times 2}$ we have:

$$\begin{aligned}\dot{s} &= \lambda\dot{\hat{x}} + \lambda_3\dot{\hat{x}}_3 = \lambda\dot{\hat{x}} + \lambda_3\left(F\dot{z} + FA\dot{\hat{x}} + FB\dot{u}\right) \\ &\quad - \lambda\dot{x}_d - \lambda_3\dot{x}_{d3}\end{aligned} \tag{40}$$

Using the equality $FB = 1$ results that:

$$\dot{s} = (\lambda + \lambda_3 FA)\dot{\hat{x}} + \lambda_3 F\dot{z} + \lambda_3\dot{u} - \lambda\dot{x}_d - \lambda_3\dot{x}_{d3} \tag{41}$$

From the observer (27) one can write:

$$\begin{aligned}\dot{s} &= (\lambda + \lambda_3 FA)(z + A\hat{x} + Bu + B\eta + \mu_2) \\ &\quad + \lambda_3 F(-z + \mu_1) + \lambda_3\dot{u} - \lambda\dot{x}_d - \lambda_3\dot{x}_{d3}\end{aligned} \tag{42}$$

Theorem 2- The following input in system (23) provides finite reaching time to the sliding surface (26).

$$\begin{aligned}\dot{u} &= -\frac{(\lambda + \lambda_3 FA)(z + A\hat{x} + Bu + B\eta + \mu_2)}{\lambda_3} \\ &\quad - \frac{\lambda_3 F(-z + \mu_1) - \lambda\dot{x}_d - \lambda_3\dot{x}_{d3} + k_1\, sign(s) + k_2\, s}{\lambda_3}\end{aligned} \tag{43}$$

where k_1 and k_2 are constant coefficients.

Proof. Equations (43) and (42) result:

$$\dot{s} = -k_1\, sign(s) - k_2\, s \tag{44}$$

Considering the Lyapunov function $V = 0.5s^2$:

$$\dot{V} = s\dot{s} = s(-k_1\, sign(s) - k_2\, s) = -k_1|s| - k_2 s^2 \le k_1|s| \tag{45}$$

Therefore, $t_f \le \frac{|s(0)|}{k_1}$ and t_f is the finite time reaching to the surface [25]. Substitution the observer inputs results:

$$\begin{aligned}\dot{u} &= -\frac{(\lambda + \lambda_3 FA)(z + A\hat{x} + Bu + B\eta + P^{-1} sign(e))}{\lambda_3} \\ &\quad - \frac{\lambda_3 F(-z + e) - \lambda\dot{x}_d - \lambda_3\dot{x}_{d3} + k_1\, sign(s) + k_2\, s}{\lambda_3}\end{aligned} \tag{46}$$

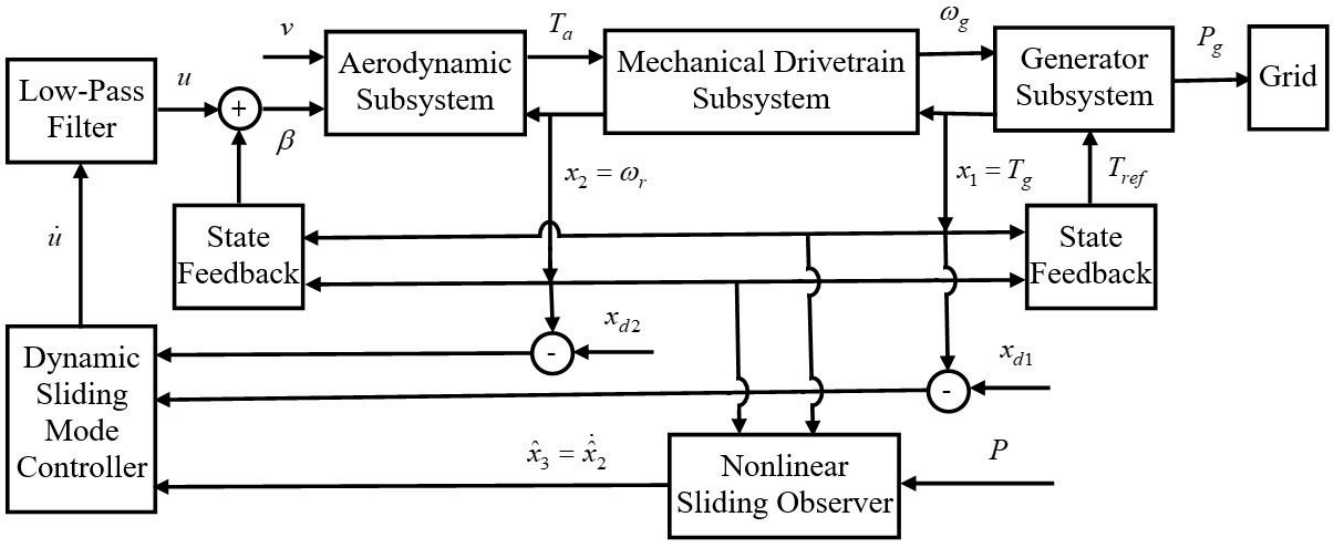


Fig. 3: The structure of the D-SMC

5.2. Design of Convectional Controller

Consider a sliding surface as:

$$s = \lambda(\hat{x} - x_d)$$
$$\lambda = [\lambda_1, \lambda_2] \in R^{1\times 2} \quad (47)$$

Using the observer (27), we have:

$$\dot{s} = \lambda\dot{\hat{x}} - \lambda\dot{x}_d = \lambda\left(z + A\hat{x} + Bu + B\eta + \mu_2\right)$$
$$-\lambda\dot{x}_d = \lambda z + \lambda A\hat{x} + \lambda Bu + \lambda B\eta + \lambda\mu_2 - \lambda\dot{x}_d \quad (48)$$

Due to the equality $\lambda B = \lambda_2$:

$$\dot{s} = \lambda z + \lambda A\hat{x} + \lambda_2 u + \lambda_2\eta + \lambda\mu_2 - \lambda\dot{x}_d \quad (49)$$

Theorem 3- The following input in system (23) provides finite reaching time to the sliding surface (47).

$$u = -\frac{\lambda z + \lambda A\hat{x} + \lambda_2\eta + \lambda\mu_2 - \lambda\dot{x}_d + k_1\, sign(s) + k_2\, s}{\lambda_2} \quad (50)$$

where k_1 and k_2 are constant coefficients.

Proof. Equations (50) and (49) result:

$$\dot{s} = -k_1\, sign(s) - k_2\, s \quad (51)$$

Considering the Lyapunov function $V = 0.5s^2$:

$$\dot{V} = s\dot{s} = s\left(-k_1\, sign(s) - k_2\, s\right) = -k_1|s| - k_2 s^2 \le k_1|s| \quad (52)$$

Therefore, $t_f \le \frac{|s(0)|}{k_1}$ and t_f is the finite time reaching to the surface [25]. Substitution the observer inputs results:

$$u = -\frac{\lambda z + \lambda A\hat{x} + \lambda_2\eta}{\lambda_2}$$
$$-\frac{\lambda P^{-1} sign(e) - \lambda\dot{x}_d + k_1\, sign(s) + k_2\, s}{\lambda_2} \quad (53)$$

6. Simulations Presentation

Based on the same NSO, two simulations are done according to the D-SMC and C-SMC approaches for a reliable comparision. In simulations the feedback parameters are selected as $a_1 = -5$ and $a_2 = -6$.

In addition the initial values are considered as zero i.e. $\hat{x}_i(0) = 0, z_i(0) = 0 : i, j = 1,2$. Moreover, the initial value of generator torque and rotor angular velocity are set to $x_1(0) = T_g(0) = -3$ and $x_2(0) = \omega_r(0) = 5$ respectively, and also $Q = I \in R^{2\times 2}$. These two approaches are applied to the 5MW two-shaft WT located at Colorado in National Renewable Energy Laboratory (NREL), with the parameters in table 1 [57]. For this turbine the optimal values for pitch blade and TSR are $\beta_{opt} = 0$ and $\lambda_{opt} = 7.55$ respectively. The WS is shown in the Fig. 4 with the mean of 7 and maximum deviation of 4.

Remark 2- In all of the following figures, the horizontal axis is time based on the second.

Table 1: The parameters of WT in NREL

Notation	Value	Unit
r	21.62	m
ρ	1.308	kg/m^3
J_r	3.25×10^5	$kg\times m^2$
J_g	34.4	$kg\times m^2$
K_r	27.36	$(N\times m)/(rad/s)$
K_g	0.2	$(N\times m)/(rad/s)$
K_{ls}	9.5×10^3	$(N\times m)/rad$
B_{ls}	2.691×10^5	$(N\times m)/(rad/s)$
n_g	43.165	$Scalar$

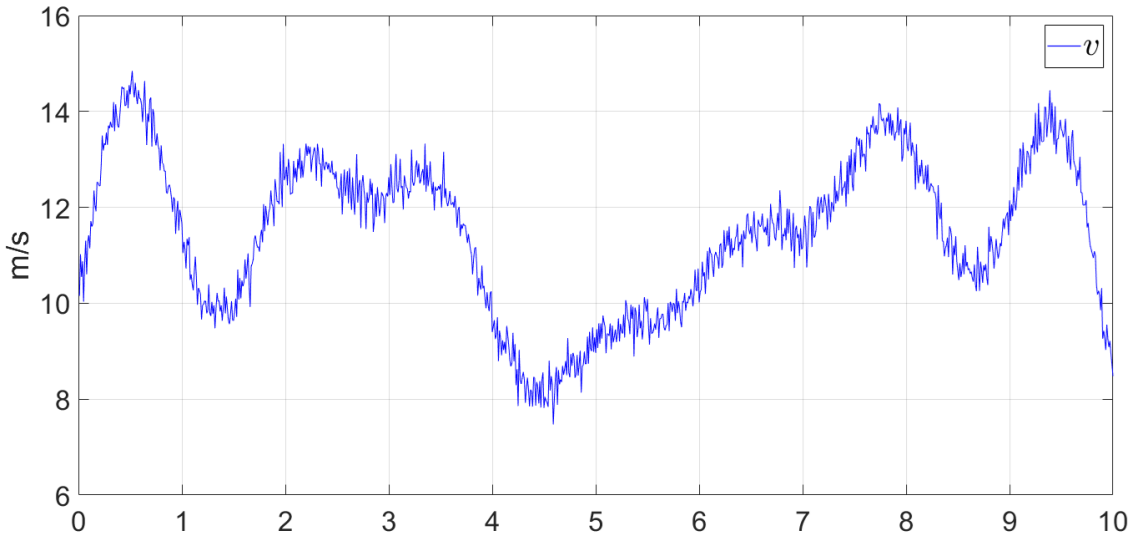


Fig. 4: Profile of WS

Example 1. The D-SMC Simulation

The simulation results are presented in Figs. 5 till 8 with the parameters of $k_1 = 2$ and $k_2 = 5$ and the surface coefficients as $\lambda = [30,3]$, $\lambda_3 = 1$. The initial value of dynamic (46) is selected as $u(0) = 0$. Figs. 5 and 6 show the generator torque and rotor angular velocity. The tracking convergence of the system states and proposed NSO are clearly observed. The finite convergence of the surface is shown in Fig. 7. The chattering-free pitch angle or controller output is shown in Fig. 8.

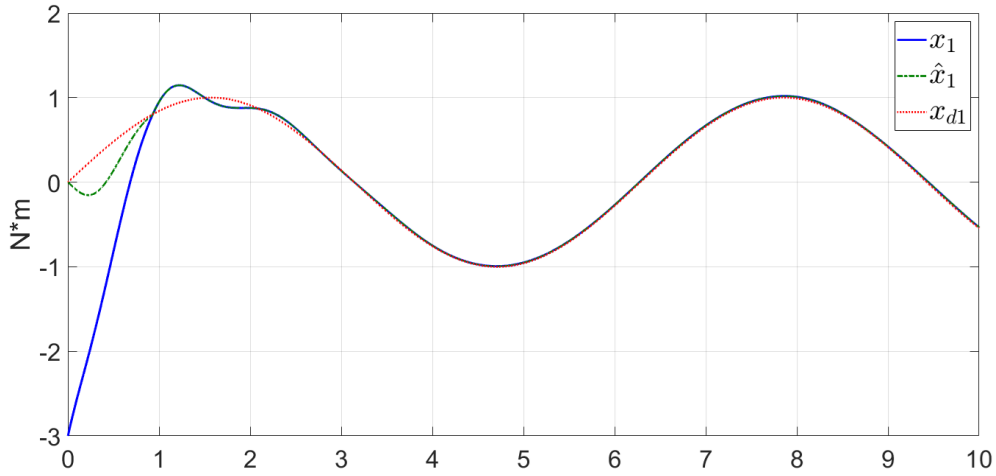


Fig. 5: D-SMC generator torque and its estimation

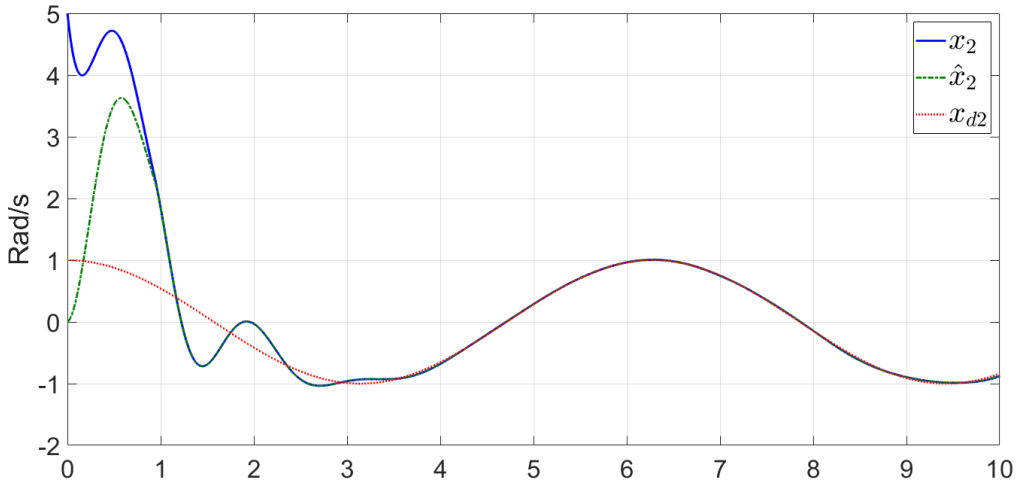


Fig. 6: D-SMC rotor angular velocity and its estimation

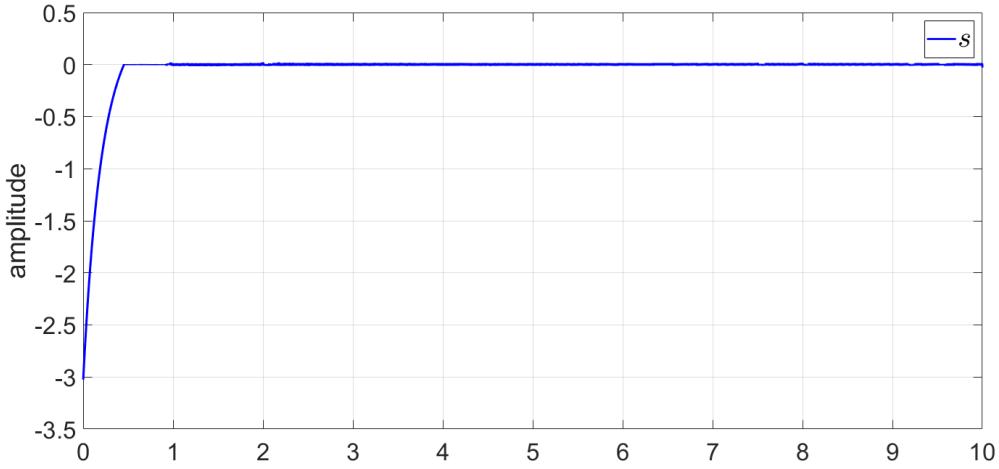


Fig. 7: D-SMC finite time zero convergence of sliding surface

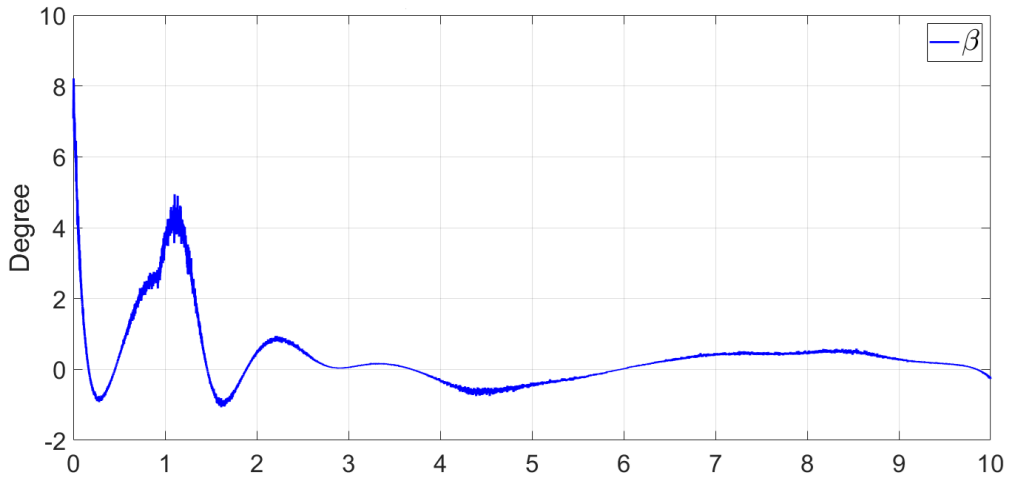


Fig. 8: D-SMC pitch angle of blades

Example 2. The C-SMC Simulation

All the parameters are set as D-SMC in the example 1, i.e the same observer with similar parameters and also $\lambda = [30,3]$ and $k_1 = 2$ and $k_2 = 5$. Then, the results of comparison between D-SMC and C-SMC are valid.

Figs. 9 till 12 are presented the simulation results. Figs. 9 and 10 show the generator torque and rotor angular velocity. The tracking convergence of the system states and proposed NSO are clearly observed. The finite time convergence of the sliding surface is shown in Fig 11. The pitch angle of the controller output is shown in Fig. 12.

The good performance of the proposed NSO and chattering-free in D-SMC are observed from these figures. Nevertheless, chattering is available in C-SMC. Moreover, the D-SMC simplicity design is remarkable.

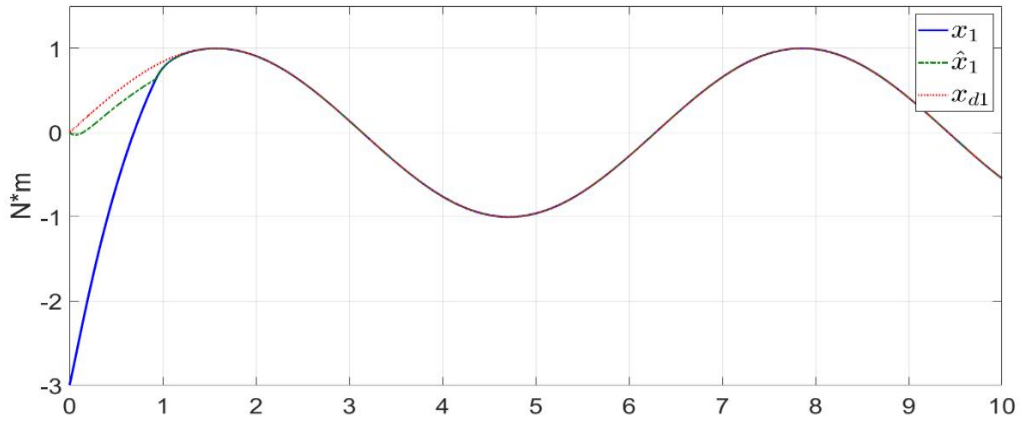


Fig. 9: C-SMC generator torque and its estimation

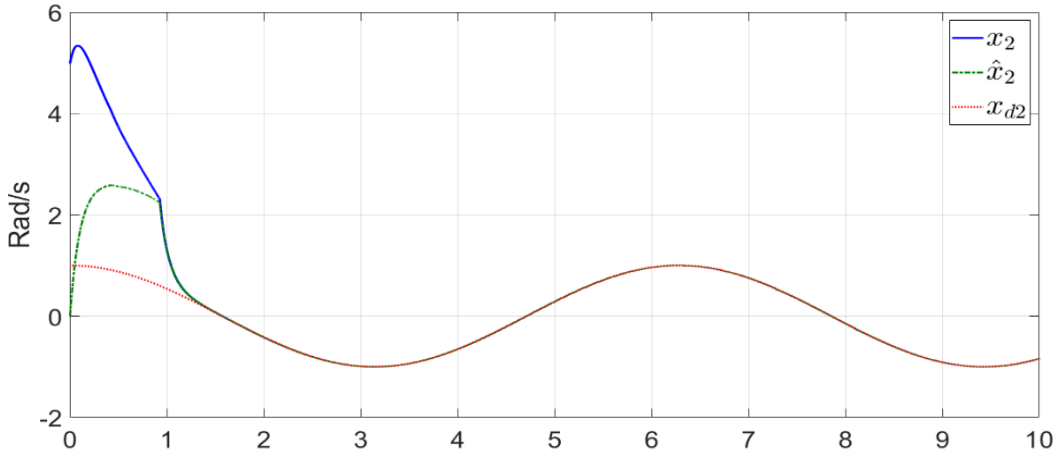


Fig. 10: C-SMC rotor angular velocity and its estimation

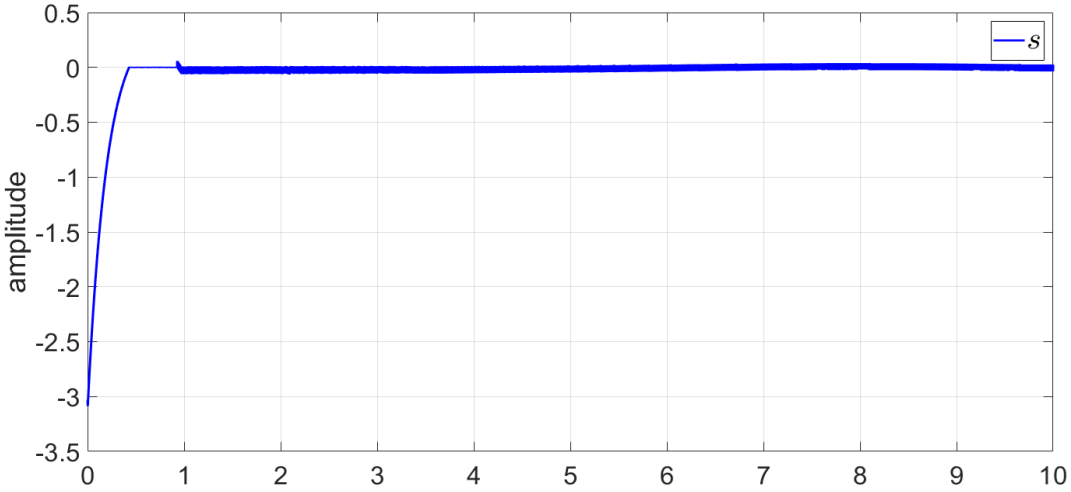


Fig. 11: C-SMC finite time zero convergence of sliding surface

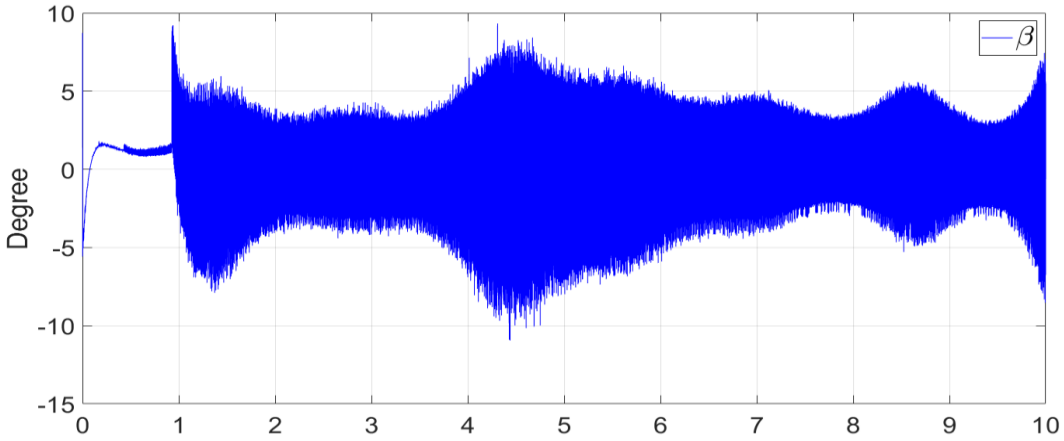


Fig. 12: C-SMC pitch angle of blades

7. Conclusion

This paper firstly provides a novel approach to enhance a smooth controller for pitch angle regulation of WT in VS turbines. At first, it proposes a chattering-free method based on D-SMC. Secondly, it presents a new design for NSO. The paper also demonstrates the closed-loop stability of D-SMC and also NSO using Lyapunov theory of stability. For practical applications, the D-SMC and NSO are integrated with state feedback to derive a linear model that considers the pitch blade angle as input. Moreover, the uncertainty of the WT model is also available in linear model. The overall closed-loop system is then compared to C-SMC with the same parameters and observer, which are used in D-SMC and therefore, comparison is reliable. Both of D-SMC and C-SMC are applied to 5MW two-shaft WT. It is shown the D-SMC approach successfully eliminates chattering, unlike the C-SMC. Additionally, the design process reveals that D-SMC is conceptually simple and easy to implement.

Credit Authorship Contribution Statement

Ali Karami-Mollaee: Conceptualization, Formal analysis, Methodology, Software, Validation, Roles/Writing - original draft, Writing - review & editing.

Declaration Of Competing Interest

The authors declare that they have no known competing financial interests or personal relationships that could have appeared to influence the work reported in this paper. The ethical issues; including plagiarism, informed consent, misconduct, data fabrication and/or falsification, double publication and/or submission, redundancy has been completely observed by the authors.

References

[1] S. Derakhshani Pour, R. Eslami, "Efficient responding to demand and robust voltage control of an islanded DC microgrid under variations in load and supply," *Journal of Applied Research in Electrical Engineering*, vol. 3, no. 1, pp. 51-63, 2024.

[2] T. Burton, D. Sharpe, N. Jenkins, E. Bossanyi, *Wind Energy Handbook*, Hoboken, NJ, Wiley, 2001.

[3] J. F. Manwell, J. McGowan, A. Rogers, *Wind Energy Explained: Theory, Design and Applications*, Hoboken, NJ, Wiley, 2002.

[4] P. W. Carlin, A. S. Laxson, E. B. Muljadi, "The history and state of the art of variable-speed wind turbine technology," *Wind Energy: An International Journal for*

Progress and Applications in Wind Power Conversion Technology, vol. 6, no. 2, pp. 129–159, 2003.
[5] Y. D. Song, B. Dhinakaran, X. Y. Bao, "Variable speed control of wind turbines using nonlinear and adaptive algorithms," *Wind Engineering and Industrial Aerodynamics*, vol. 85, no. 3, pp. 293–308, 2000.
[6] H. R. Safa, A. A. Ghadimi, M. R. Miveh, "assessing power system adequacy and generation expansion planning inthe presence of wind power plants considering uncertainties in the DIgSILENT software environment," *Journal of Applied Research in Electrical Engineering*, vol. 3, no. 1, pp. 99-109, 2024.
[7] M. Rahimi, M. Parniani, "Dynamic behavior and transient stability analysis of fixed speed wind turbines," *Renewable Energy*, vol. 34, no. 12, pp. 2613–2624, 2009.
[8] A. Sumper, O. Gomis-Bellmunt, A. Sudri-Andreu, R. Villafafila-Robles, J. Rull-Duran, "Response of fixed speed wind turbines to system frequency disturbances," *IEEE Transaction on Power Systems*, vol. 24, no. 1, pp. 181–192, 2009.
[9] K. Ghedamsi, D. Aouzellag, E. M. Berkouk, "Control of wind generator associated to a flywheel energy storage system," *Renewable Energy*, vol. 33, no. 9, pp. 2145–2156, 2008.
[10] I. Poultangari, R. Shahnazi, M.Sheikhan, "RBF Neural network based PI pitch controller for a class of 5-MW wind turbines using particle swarm optimization algorithm," *ISA Transactions*, vol. 51, no. 5, pp. 641–648, 2012.
[11] F. D. Bianchi, H. D. Battista, R. J.Mantz, *Wind turbine control systems: principles, modelling and gain scheduling design*, London, Springer-Verlag, 2007.
[12] H. Camblong, "Digital robust control of a variable speed pitch regulated wind turbine for above rated wind speeds," *Control Engineer Practice*, vol. 16, no. 8, pp. 946-958, 2008.
[13] A. Asgharniaa, R. Shahnazi, A. Jamali, "Performance and robustness of optimal fractional fuzzy PID controllers for pitch control of a wind *turbine using chaotic optimization algorithms," ISA* Transactions, vol. 79, pp. 27 – 44, 2018.
[14] K. Oh, J. Park, J. Lee, J. Lee, "Implementation of a torque and a collective pitch controller in a wind turbine simulator to characterize the dynamics at three control regions," *Renewable Energy*, vol. 79, pp. 150-160, 2015.
[15] A. Hatami, B. Moetakef-Imani, "Innovative adaptive pitch control for small wind turbine fatigue load reduction," *Mechatronics*, vol. 40, pp. 137–145, 2016.
[16] Y. Yuan, J. Tang, "Adaptive Pitch Control of Wind Turbine for Load Mitigation under Structural Uncertainties," *Renewable Energy*, vol. 105, pp. 483-494, 2017.
[17] R. Gao, Z. Gao, "Pitch control for wind turbine systems using optimization, estimation and compensation," *Renewable Energy*, vol. 91, pp. 501-515, 2016.
[18] L. Chen, Y. Yang, Y. Gao, Z. Gao, Y. Guo, L. Sun, "A novel real-time feedback pitch angle control system for vertical-axis wind turbines," *Journal of Wind Engineering and Industrial Aerodynamics*, vol. 195, pp. 104023, 2019.
[19] Y. Yuan, X. Chen, J. Tang, "Multivariable robust blade pitch control design to reject periodic loads on wind turbines," *Renewable Energy*, vol. 146, pp. 329-341, 2020.
[20] A. Lasheen, M. Elnaggar, H. Yassin, "Adaptive control design and implementation for collective pitch in wind energy conversion systems," *ISA Transactions*, vol. 102, pp. 251, 2020.
[21] M. Rahimi, M. Asadi, "Control and dynamic response analysis of full converter wind turbines with squirrel cage induction generators considering pitch control and drive train dynamics," *Electrical Power and Energy Systems*, vol. 108, pp. 280–292, 2019.
[22] B. Boukhezzar, L. Lupu, L. Lupu, M. Hand, "Multivariable control strategy for variable speed, variable pitch wind turbines, *Renewable Energy*, vol. 32, no. 8, pp. 1273–1287, 2007.
[23] M. Abolvafaei, S. Ganjefar, "Maximum power extraction from a wind turbine using second-order fast terminal sliding mode control," *Renewable Energy*, vol. 139, pp. 1437-1446, 2019.
[24] J. J. E Slotine, W. Li, *Applied Nonlinear Control*, Prentice Hall, Englewood Cliffs, 1991.
[25] A. Karami-Mollaee, N. Pariz, H. M. Shanechi, "Position control of servomotors using neural dynamic sliding mode, Journal of Dynamic Systems," *Measurement, and Control*, vol. 133, no. 6, pp. 141-150, 2011.
[26] W. Perruquetti, J. Pierre-Barbot, *Sliding mode control in engineering*, Marcel Dekker, 2002.
[27] F. Golnary, H. Moradi, "Design and comparison of quasi continuous sliding mode control with feedback linearization for a large scale wind turbine with wind speed estimation," *Renewable Energy*, vol. 127, pp. 495-508, 2018.
[28] F. Golnary, H. Moradi, "Dynamic modelling and design of various robust sliding mode controls for the wind turbine with estimation of wind speed," *Applied Mathematical Modelling*, vol. 65, pp. 566-585, 2019.
[29] R. F. Nayeh, H. Moradi, G. Vossoughi, "Multivariable robust control of a horizontal wind turbine under various operating modes and uncertainties: A comparison on sliding mode and H-infinity control," *Electrical Power and Energy Systems*, vol. 115, pp. 105474, 2020.
[30] A. Cetrini, F. Cianetti, M.L. Corradini, G. Ippoliti, G. Orlando, "On-line fatigue alleviation for wind turbines by a robust control approach," *Electrical Power and Energy Systems*, vol. 109, pp. 384–394, 2019.
[31] L. Colombo, M. L. Corradini, G. Ippoliti, G. Orlando, "Pitch angle control of a wind turbine operating above the rated wind speed: A sliding mode control approach, ISA Transactions, vol. 96, pp. 95, 2020.
[32] X. Yin, W. Zhang, Z. Jiang, L. Pan, "Adaptive robust integral sliding mode pitch angle control of an electro-hydraulic servo pitch system for wind turbine," *Mechanical Systems and Signal Processing*, vol. 133, pp. 105704, 2019.
[33] B. Torchani, A. Sellami, G. Garcia, "Variable speed wind turbine control by discrete-time sliding mode approach," *ISA Transactions*, vol. 62, pp. 81-86, 2016.
[34] H. Lee, V-I Utkin, "Chattering suppression methods in sliding mode control systems," *Annual Review in Control*, vol. 31(2), pp. 179-188, 2007.

[35] C.-C. Fuh, "Variable-thickness boundary layers for sliding mode control," *Journal of Marine Science and Technology*, vol. 16, no. 4, pp. 288–294, 2008.
[36] H.-M. Chen, J.-C. Renn, J.-P. Su, "Sliding mode control with varying boundary layers for an electro-hydraulic position servo system," *The International Journal of Advanced Manufacturing Technology*, vol. 26, no. 1-2, pp. 117–123, 2005.
[37] X. Zhang, "Sliding mode-like fuzzy logic control with adaptive boundary layer for multiple-variable discrete," *Journal of Intelligent Systems*, vol. 25, no. 2, pp. 209–220, 2016.
[38] H. Allamehzadeh, J. Y. Cheung, "Optimal fuzzy sliding mode control with adaptive boundary layer," *WSEAS Transaction on Systems*, vol. 3, no. 5, pp. 1887–1892, 2004.
[39] M. Cucuzzella, G. P. Incremona, A. Ferrara, "Design of robust higher order sliding mode control for micro grids," *IEEE Journal on Emerging and Selected Topics in Circuits and Systems*, vol. 5, no. 3, pp. 393–401, 2015.
[40] R. Nonaka, Y. Yamashita, D. Tsubakino, "General scheme for design of higher-order sliding-mode controller," *American Control Conference (ACC)*, pp. 5176–5181, 2015.
[41] A. J. Koshkouei, K. J. Burnham, A. S. Zinober, "Dynamic sliding mode control design," *IEE Proceedings-Control Theory and Applications*, vol. 152, no. 4, pp. 392–396, 2005.
[42] M.-S. Chen, C.-H. Chen, F.-Y. Yang, "An LTR-observer based dynamic sliding mode control for chattering reduction," *Automatica*, vol. 43, no. 6, pp. 1111–1116, 2007.
[43] A. Karami-Mollaee, A. A. Shojaei, O. Barambones, M. F. Othman "Dynamic sliding mode control of pitch blade wind turbine using sliding mode observer," *Transactions of the Institute of Measurement and Control*, vol. 44, no. 15, pp. 3028-3038, 2022.
[44] A. Levant, "Sliding order and sliding accuracy in sliding mode control," *International Journal of Control*, vol. 58, no. 6, pp. 1247–1263, 1993.
[45] A. Levant, "Homogeneity approach to high-order sliding mode design," *Automatica*, vol. 41, no. 5, pp. 823–830, 2005.
[46] F. Plestan, A. Glumineau, S. Laghrouche, "A new algorithm for high-order sliding mode control," *International Journal of Robust and Nonlinear Control*, vol. 18, no. 4–5, pp. 441–453, 2008.
[47] Y. B. Shtessel, L. Fridman, A. Zinober, "Higher order sliding modes," *International Journal of Robust and Nonlinear Control*, vol. 18, no. 4–5, pp. 381–384, 2008.
[48] Y. Yang, S. Qin, P. Jiang, "A modified super-twisting sliding mode control with inner feedback and adaptive gain schedule," *International Journal of Adaptive Control and Signal Processing*, vol. 31, no. 3, pp. 398–416, 2017.
[49] Y.-T. Liu, T.-T. Kung, K.-M. Chang, S.-Y. Chen, "Observer-based adaptive sliding mode control for pneumatic servo system," *Precision Engineering*, vol. 37, no. 3, pp. 522–530, 2013.
[50] Y. Xia, Z. Zhu, M. Fu, "Back-stepping sliding mode control for missile systems based on an extended state observer," *IET Control Theory and Application*, Vol. 5, no. 1, pp. 93–102, 2011.
[51] C. Fuyang, W. Lei, K. Zhang, G. Tao, B. Jiang, "A novel nonlinear resilient control for a quadrotor UAV via backstepping control and nonlinear disturbance observer," *Nonlinear Dynamics*, vol. 85, no. 2, pp. 1281–1295, 2016.
[52] Q. R. Butt, A. I. Bhatti, M. R. Mufti, M. A. Rizvi, I. Awan, "Modeling and online parameter estimation of intake manifold in gasoline engines using sliding mode observer," *Simulation Modelling Practice and Theory*, vol. 32, pp. 138–154, 2013.
[53] J. Davila, L. Fridman, A. Levant, "Second-order sliding mode observer for mechanical systems," *IEEE Transactions on Automatic Control*, vol. 50, no. 11, pp. 1785–1789, 2005.
[54] Y. Xiong, M. Saif, "Sliding mode observer for nonlinear uncertain systems," *IEEE Transactions on Automatic Control*, vol. 46, no. 12, pp. 2012–2017, 2001.
[55] A. Benchaib, A. Rachid, E. Audrezet, M. Tadjine, "Real time sliding-mode observer and control of an induction motor," *IEEE Transactions on Industrial Electronics*, vol. 46, no. 1, pp. 128–138, 1999.
[56] B. Boukhezzar, H. Siguerdidjane, "Nonlinear control of a variable-speed wind turbine using a two-mass model," *IEEE on Energy Conversion*, vol. 26, no. 1, pp. 149-162, 2010.
[57] E. A. Bossanyi, A. D. Wright, P. A. Fleming, Controller field tests on the NREL CART2 turbine, No. NREL/TP-5000-49085, *National Renewable Energy Lab* (NREL), Golden, CO (United States), 2010.

BIOGRAPHY



Ali Karami-Mollaee, was born in 1980 in Mashhad, Iran and received the B.Sc. in electrical engineering from Ferdowsi University of Mashhad in 2002. He is received the M.Sc. in electrical engineering from Tarbiyat Modarres University of Tehran, Iran in 2005 and Ph.D in control engineering from Ferdowsi University of Mashhad, Iran in 2010. At present he is associate professor in Hakim Sabzevari University, Iran. His research interests include nonlinear and adaptive control, intelligent systems and renewable energy.

Copyrights
© 2026 by the author(s). Licensee Shahid Chamran University of Ahvaz, Ahvaz, Iran. This article is an open-access article distributed under the terms and conditions of the Creative Commons Attribution –NonCommercial 4.0 International (CC BY-NC 4.0) License (http://creativecommons.org/licenses/by-nc/4.0/).